Elimination of C/EBPα through the ubiquitin-proteasome system promotes the development of liver cancer in mice

Guo-Li Wang, Xiurong Shi, Simon Haefliger, Jingling Jin, Angela Major, Polina Iakova, Milton Finegold, and Nikolai A. Timchenko

Department of Pathology and Immunology and Huffington Center on Aging, Baylor College of Medicine, Houston, Texas, USA.

Despite significant advancements in our understanding of cancer development, the molecular mechanisms that underlie the formation of liver cancer remain largely unknown. C/EBPα is a transcription factor that regulates liver quiescence. Phosphorylation of C/EBPα at serine 193 (S193-ph) is upregulated in older mice and is thought to contribute to age-associated liver dysfunction. Because development of liver tumors is associated with increasing age, we investigated the role of S193-ph in the development of liver cancer using knockin mice expressing a phospho-mimetic aspartic acid residue in place of serine at position 193 (S193D) of C/EBPα. The S193D isoform of C/EBPα was able to completely inhibit liver proliferation in vivo after partial hepatectomy. However, treatment of these mice with diethylnitrosamine/phenobarbital (DEN/PB), which induces formation of liver cancer, actually resulted in earlier development of liver tumors. DEN/PB treatment was associated with specific degradation of both the S193-ph and S193D isoforms of C/EBPα through activation of the ubiquitin-proteasome system (UPS). The mechanism of UPS-mediated elimination of C/EBPα during carcinogenesis involved elevated levels of gankyrin, a protein that was found to interact with the S193-ph isoform of C/EBPα and target it for UPS-mediated degradation. This study identifies a molecular mechanism that supports the development of liver cancer in older mice and potential therapeutic targets for the prevention of liver cancer.

Introduction

Liver is a quiescent tissue that is able to regenerate itself in response to partial hepatectomy (PH) and after injury (1, 2). Under normal conditions, the quiescent stage of the liver is mediated by C/EBP proteins (3) and by Rb family proteins (4). A member of the C/EBP family, transcription factor C/EBPα, is expressed at high levels in liver and is a critical regulator of many metabolic processes (3). The constitutional deletion of the C/EBPα gene causes mice to die shortly after birth due to impaired energy homeostasis (5). Numerous studies have shown that C/EBPα supports liver quiescence (3, 6–9). While the energy metabolism and expression of liver-specific genes are controlled by transcriptional activity of C/EBPα, the growth inhibitory activity of C/EBPα is mediated by direct interactions of C/EBPα with cell-cycle proteins (8–11). It has been shown that C/EBPα utilizes different mechanisms in different tissues. C/EBPα growth inhibitory activity in liver of young animals is mediated through direct interactions with cdk2 (8–11). In adipose and myeloid tissues, the antiproliferative effects of C/EBPα are mediated through repression of E2F-dependent transcription (12). C/EBPα also interacts with several chromatin-remodeling proteins. It has been shown that C/EBPα cooperates with the catalytic components of SWI/SNF complex, Brm and Brg1, in the regulation of gene expression during adipogenesis (13). Following these findings, we and other groups have observed that C/EBPα interacts with Brm and that this interaction is involved in the inhibition of liver proliferation and in the inhibition of proliferation of cultured cells (11, 14–16). Recent studies have shown a critical role of C/EBPα in development of aging phenotype in the liver. Aging liver hyperphosphorylates C/EBPα at S193 and increases amounts of the age-specific C/EBPα-Brm complex, which represses E2F-dependent promoters and inhibits liver proliferation (11, 14, 15). Our recent studies show that the phosphorylation of C/EBPα at S193 enhances the interactions of C/EBPα with histone deacetylase 1 (HDAC1) and with heterochromatin protein 1α (HP1α) and that this interaction is a key event in the inhibition of liver proliferation of old mice (17, 18).

Despite the elevation of the C/EBPα-Brm-HDAC1 complex and following epigenetic silencing of E2F-dependent promoters, livers of old mice frequently develop tumors beginning at 22–24 months of age. We generated C/EBPα-S193D knockin mice, which express the constitutively "active," age-specific isoform of C/EBPα. These studies allowed us to identify a molecular basis for liver cancer. Although the S193D-C/EBPα strongly inhibits liver proliferation after PH, we found that the S193D knockin mice developed liver cancer much earlier than WT mice. The molecular mechanisms of the early liver cancer in these knockin mice and in old mice included the complete elimination of the S193D and S193-ph isoforms of C/EBPα by activation of the gankyrin-UPS (where UPS indicates *ubiquitin-proteasome system*) pathway.

Results

Generation of C/EBPα-S193D knockin mice and characterization of liver functions. In livers of old mice, the major portion of C/EBPα is phosphorylated at S193 (10, 15). The ph-S193 isoform of C/EBPα is the strong inhibitor of cell proliferation in tissue culture models, and the phosphorylation of S193 correlated with the inhibition of liver proliferation (10, 15, 19). Despite these observations, the causal role of phosphorylation of S193 in the regulation of liver biology has been not shown. To examine the role of ph-S193 isoform of C/EBPα in liver proliferation and in regulation of the age-associated dysfunctions of the liver, we generated C/EBPα-S193D
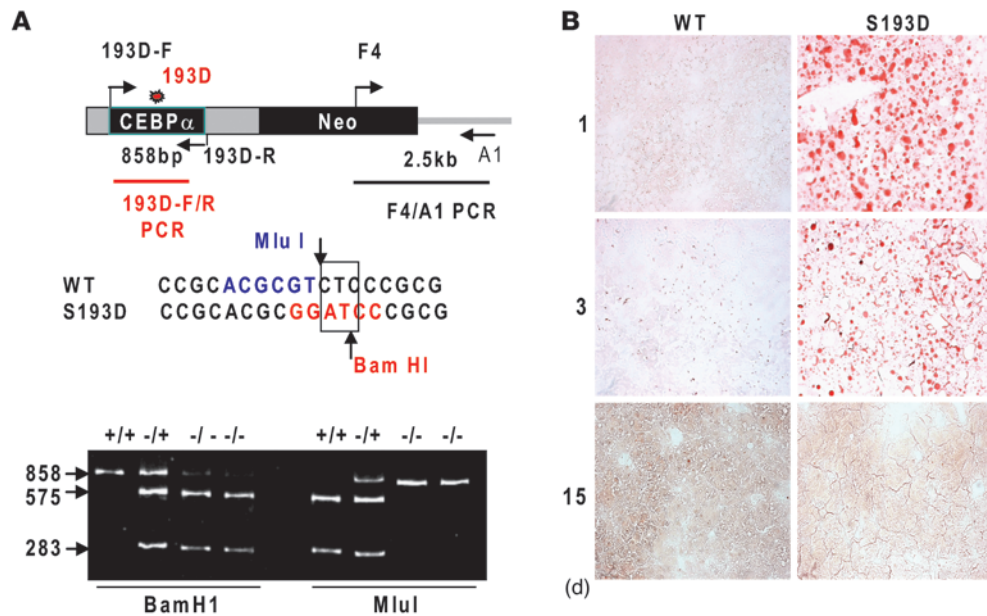
Figure 1
Generation of C/EBPα-S193D mice and characterization of liver functions in these animals. (**A**) Genotyping of C/EBPα-S193D mice. Upper image shows a structure of the targeting construct and positions of primers used for genotyping. Primers 193D-F and 193D-R were used for generation of PCR products and following restriction with MluI and BamHI. Middle image shows the sequence surrounding S193. TC nucleotides were mutated to GA, leading to the disruption of the restriction site for MluI and creation of restriction site for BamHI. Bottom image shows an example of genotyping. PCR products of 858 bp were generated using DNA from littermates and examined by restriction with MluI and BamHI. (**B**) Oil red O staining of the liver of WT and C/EBPα-S193D mice at days 1, 3, and 15 after birth. Original magnification, ×20.

knockin mice that express the age-specific C/EBPα isoform. We replaced WT C/EBPα with the mutant gene as it is shown in Figure 1A. C/EBPα knockin construct contained a substitution of TC to GA in the position of S193 (Figure 1A). This substitution leads to the mutation of Ser to Asp and to alterations in restriction sites for MluI and BamH1. Therefore, PCR products from WT animals are resistant to BamHI, but are sensitive to MluI, while PCR products from homozygous knockin mice are cut by BamHI, but not by MluI. Figure 1A shows a typical genotyping of a litter that contained WT, heterozygous, and homozygous mice. To confirm this genotyping, the PCR products were sequenced (Supplemental Figure 1A; supplemental material available online with this article; doi:10.1172/JCI41933DS1). The animals were born at the expected Mendelian frequency; and the homozygous and heterozygous mice did not show abnormal growth within 1 year. In this paper, we bred heterozygous mice and used WT, heterozygous, and homozygous littermates for the majority of studies.

Since C/EBPα is involved in the regulation of fat accumulation, we stained livers of S193D mice and WT mice with oil red O. These studies have found that S193D mutation leads to the accumulation of fat droplets in the livers of S193D mice at very early ages (days 1 and 3 after birth), while WT livers do not have fat droplets at that time (Figure 1B). We next asked whether the liver functions are affected by the S193D mutation. The analysis of blood parameters showed significant elevations in activities of alanine and aspartate transaminases, ALT and AST, and the elevation of levels of triglycerides (Table 1). These alterations are similar to those observed in livers of old mice (10), showing

that the S193D mutation mimics the functions of S193-ph isoform of C/EBPα in livers of old mice. In addition to these alterations, we also found that levels of glucose are reduced in the blood of S193D mice. Other blood parameters do not differ or show minor alterations.

C/EBPα-S193D isoform inhibits liver proliferation after PH. Since the ph-S193-C/EBPα isoform is abundant in livers of old mice and is required for the inhibition of liver proliferation (15), we suggested that these animals should be resistant to the development of tumors. Therefore, we tested this hypothesis using a well-established protocol of carcinogenesis: diethylnitrosamine/phenobarbital (DEN/PB). Prior to these studies, we examined proliferative capacities of liver in young adult S193D mice after PH. PHs were performed in 2-month-old WT and S193D mice. BrdU labeling showed that a peak of DNA synthesis in WT mice is observed at 36 hours after PH. However, DNA synthesis was almost completely blocked in C/EBPα-S193D mice (Figure 2, A and B). Examination of mitotic figures showed that mitotic figures are virtually undetectable in knockin mice (Figure 2C). Investigations of the livers at 72 hours after PH did not detect BrdU uptake and/or mitotic figures in either WT or C/EBPα-S193D knockin mice, showing that proliferation is not delayed, but rather dramatically inhibited by the mutant C/EBPα-S193D. Examination of cell-cycle proteins confirmed this conclusion. The expression of proliferating cell nuclear antigen (PCNA), cyclin D1, cyclin A, cyclin E, and cdc2 was increased in WT livers at 36–48 hours after PH; however, livers of C/EBPα-S193D mice fail to increase expression of these cell-cycle proteins (Figure 2D). Since previous studies showed that C/EBPα inhibits liver proliferation via cdk2, we examined the C/EBPα-cdk2 complexes in livers of WT and C/EBPα-S193D mice at 24 hours after PH. Significantly higher amounts of cdk2 are associated with C/EBPα in quiescent livers of C/EBPα-S193D mice than in those of WT mice. Most important, cdk2 remains associated with C/EBPα in C/EBPα-S193D mice 24 hours after PH, while no cdk2 is detectable in C/EBPα IPs from WT livers (Figure 2E). We next asked whether the C/EBPα-S193D mutant inhibits liver proliferation in heterozygous C/EBPα-S193D mice, which express 50% of constitutively active C/EBPα. Examination of mitosis and cell-cycle proteins revealed that the C/EBPα-S193D mutant also inhibits proliferation of hepatocytes in livers of heterozygous mice (Supplemental Figure 1, B and C).

Given almost complete inhibition of proliferation in C/EBPα-S193D mice within 72 hours after PH, we asked whether the liver might recover the original size in these animals at later time

Table 1
The blood chemistry of 2-month-old WT and C/EBPα-S193D knockin mice

Blood parameters	WT mice	S193D mice
ALT (U/l)	**49.4 ± 15.4**	**78.1 ± 26.3**
AST (U/l)	**102.2 ± 17.8**	**209.2 ± 77.9**
ALP (U/l)	52.4 ± 21.8	52.7 ± 21.1
T.Bill (mg/dl)	0.12 ± 0.05	0.17 ± 0.05
D.Bill (mg/dl)	0.012 ± 0.009	0.022 ± 0.023
LDH (U/L)	455.6 ± 141	620.7 ± 259.5
Alb (g/dl)	2.75 ± 0.3	2.71 ± 0.35
TP (g/dl)	4.2 ± 0.13	4.4 ± 0.35
Globulin	1.54 ± 0.16	1.54 ± 0.19
A/G Ratio	2.03 ± 0.7	1.75 ± 0.4
VLDL	11.4 ± 2.8	16 ± 6.1
Chol (mg/dl)	113 ± 10.5	98.8 ± 16.3
Trig (mg/dl)	**54.2 ± 13.8**	**80 ± 30.5**
HDL (mg/dl)	98.6 ± 15.3	81 ± 14
LDL (mg/dl)	13.6 ± 3.4	8 ± 2.2
Glucose (mg/dl)	**238.6 ± 23.9**	**178.9 ± 23**

The table shows a summary of analyses of 8 animals of each genotype. Significant alterations are shown in bold.

points after surgery. For these studies, liver mass was determined at 3, 6, 9, and 15 days after PH in WT and in S193D mice. Figure 2F shows that livers in WT animals completely restored original size at 15 days after surgery. On the contrary, S193D livers had increased weight only to 65%–70% at day 6 and then stayed at this level to the end of the experiments. We suggest that the partial restoration of the mass of S193D livers might be due to proliferation of nonhepatic cells or due to increased translation of proteins without liver proliferation. Taken together, the studies of liver regeneration have shown that the C/EBPα-S193D livers do not proliferate after PH and fail to restore the original size.

Development of tumors is accelerated in C/EBPα-S193D knockin mice. Given the strong inhibition of liver proliferation after PH in S193D knockin mice, we expected that these animals should be resistant to the development of tumors. To test this suggestion, we applied DEN/PB tumor liver induction protocol (8). We surprisingly found that the S193D mice developed tumors much earlier than WT mice (Figure 3A). The tumor formation was observed in S193D mice at 25 weeks after initiation of DEN/PB protocol (see bigger images of the tumor in Supplemental Figure 2), while in WT mice, liver tumors were detected at 35 weeks. We also found enlarged livers in S193D mice starting from 20 weeks after initiation of carcinogenesis by DEN/PB, while enlarged livers were observed in WT mice at 30 weeks. To further confirm the increased liver proliferation and early tumor formation in S193D mice, 2 additional approaches were used. First, we examined DNA synthesis by measuring BrdU uptake. BrdU was injected in animals 2–4 hours before animals were sacrificed. BrdU staining showed that DNA synthesis was increased at 25 weeks in S193D mice, while it was very rare in WT mice until 30–35 weeks (Figure 3B and see Supplemental Figure 3A). The percentage of BrdU-positive hepatocytes was higher in S193D mice at all stages of liver cancer development (Figure 3B). Second, we examined expression of cell-cycle proteins in livers of WT and S193D mice at 25 weeks after DEN injection. We found that expression of cyclin A, cyclin D1, and PCNA was significantly increased in livers of S193D mice

treated with DEN/PB, while these proteins were not detectable in livers of DEN/PB-treated WT mice at this stage (Figure 3C). Examination of C/EBPα surprisingly showed that both isoforms of S193D-C/EBPα (42 kDa and 30 kDa) were virtually not detectable in livers of S193D mice at 25 weeks after DEN/PB injection and that WT C/EBPα was also reduced at that time point (Figure 3C). Therefore, we performed detailed examination of C/EBPα in WT and S193D livers during cancer development.

Liver cancer eliminates S193D and S193-ph isoforms of C/EBPα. Given the early development of tumors in livers of S193D mice, we examined expression of C/EBPα in WT and in S193D mice at different time points after DEN/PB treatments. We found that the mutant C/EBPα-S193D was eliminated in DEN/PB-treated mice at 6 weeks after initiation, while the WT C/EBPα was gradually reduced and completely eliminated only at 30 weeks (Figure 3D). We determined levels of C/EBPα mRNA and found that DEN/PB did not affect levels of mRNA (Supplemental Figure 3B). Thus, these studies showed that liver tumor development requires specific degradation of S193D isoform in S193D knockin mice and perhaps ph-S193 isoform in WT mice. These studies suggested that, in WT animals, there is a pathway that converts C/EBPα into the S193-ph isoform and leads to degradation of the ph-S193-C/EBPα at 25–35 weeks. Searching for a kinase that might convert C/EBPα into the ph-S193 isoform, we found that DEN/PB elevates cdc2 at 30 weeks after DEN/PB treatment (Figure 3D). We next examined expression of cdc2 at early time points and found that cdc2 is elevated in both WT and S193D mice at 6 weeks and at later time points (Supplemental Figure 3C). Since our hypothesis suggested that C/EBPα is hyperphosphorylated at S193 before degradation, we examined cdc2 expression and phosphorylation of C/EBPα at an additional time point, 1 week after DEN injection. Western blotting showed that C/EBPα is not reduced, but cdc2 is already activated in livers of WT mice at 1 week after DEN injection (Figure 3E). Co-IP studies showed that cdc2 strongly interacts with WT C/EBPα at 1 and 6 weeks after DEN injection (Figure 3E). The interaction of cdc2 with C/EBPα is not detectable at later time points, perhaps due to degradation of C/EBPα. We also examined S193-ph isoform of C/EBPα in C/EBPα IPs and found that the amounts of phosphorylated C/EBPα (as a ratio to total protein) are dramatically increased at 1 and 6 weeks after DEN injection. Thus, these studies showed that C/EBPα is hyperphosphorylated at S193 by cdc2 prior to being degraded. A search for cdc2 phosphorylation site(s) within C/EBPα molecule found high scores for S193 and S21 (Figure 3F). To determine whether cdc2 phosphorylates C/EBPα at these residues, we generated 3 C/EBPα mutants S21A, S193A, and double-mutant S21A-S193A and examined phosphorylation of these mutants by cdc2, precipitated from liver tumors at 30 weeks after DEN treatments. Figure 3G shows that cdc2-dependent phosphorylation of C/EBPα is dramatically reduced by S193A mutation, S21A mutation, and double mutations. Thus, these studies revealed that cdc2 phosphorylates C/EBPα at S21 and at S193 in in vitro kinase assays.

Phosphorylation of C/EBPα by cdc2 inhibits proliferation of hepatocytes under normal conditions. Given the cdc2-mediated phosphorylation of C/EBPα at S193, one would assume that this phosphorylation should increase growth inhibitory activity of C/EBPα under conditions in which C/EBPα is not degraded. To test this hypothesis, we performed a number of experiments in cultured cells and in livers. WT C/EBPα and S193A mutant C/EBPα were cotransfected with cdc2 into Hep3B2, and phosphorylation of C/EBPα at S193 was
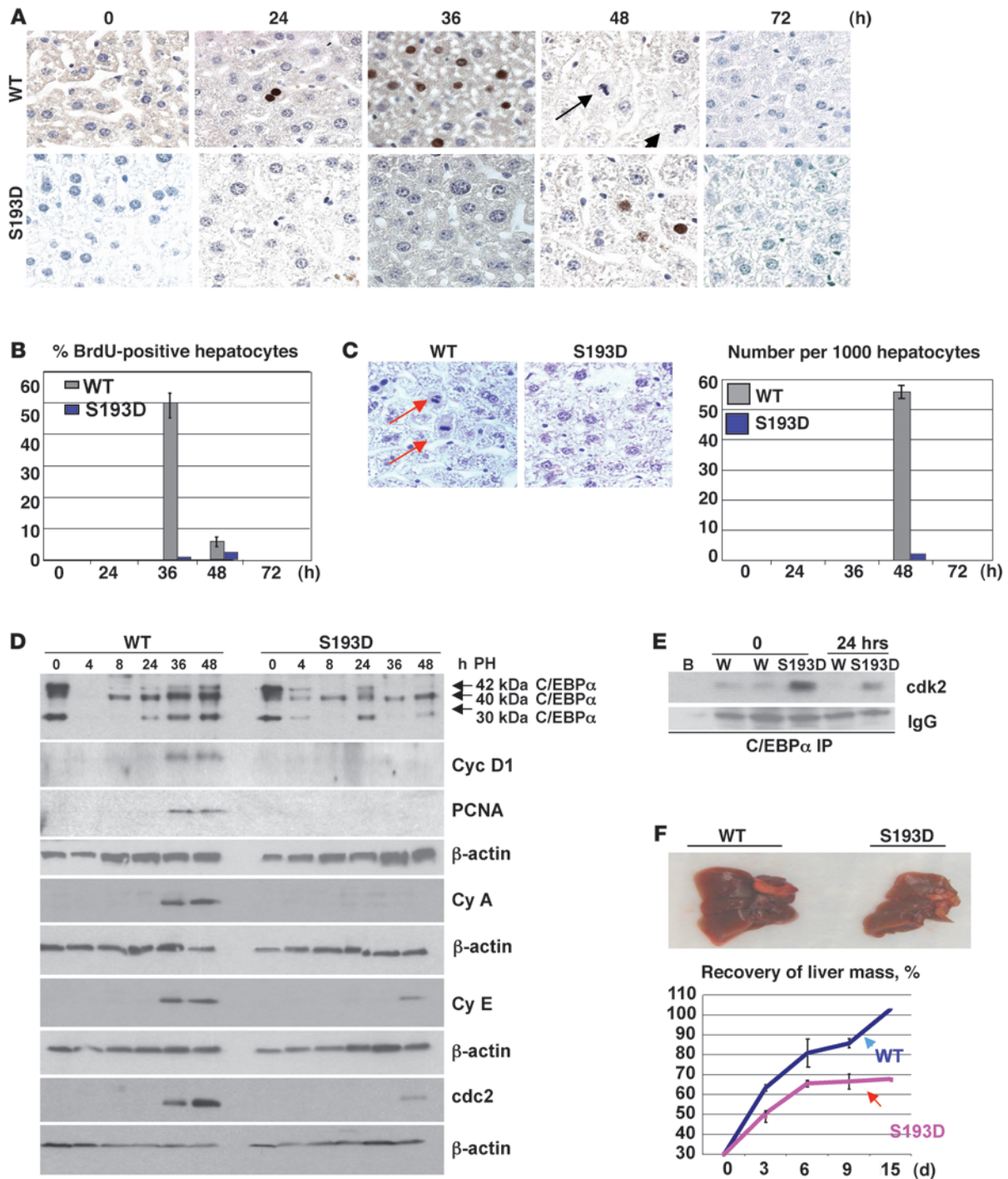
Figure 2
C/EBPα-S193D inhibits liver proliferation after PH. (**A**) C/EBPα-S193D inhibits DNA synthesis after PH. BrdU staining is shown. Arrows show mitotic figures in the liver of WT mice at 48 hours after PH. Original magnification, ×63. (**B**) Bar graphs show the percentage of BrdU-positive hepatocytes. (**C**) C/EBPα-S193D inhibits mitosis. Livers were stained with H&E. Typical pictures of mitotic figures at 48 hours after PH are shown. Original magnification, ×63. Arrows show mitotic figures. Bar graph picture shows number of mitotic figures at each time point after PH. (**D**) Expression of C/EBPα and cell-cycle proteins after PH. Positions of C/EBPα isoforms are shown on the right. Expression of cell-cycle proteins cyclin D1 (Cyc D1), PCNA, cyclin A (Cy A), cyclin E (Cy e) and cdc2 was examined with antibodies shown on the right. Each membrane was reprobed with β-actin. (**E**) C/EBPα-S193D is associated with cdk2 after PH. C/EBPα was IP from nuclear extracts and the IPs were probed with Abs to cdk2. IgG, heavy chains of immunoglobulins. B, incubation of protein with beads; W, incubation of liver proteins from WT mice with C/EBPα IgGs. (**F**) Livers of C/EBPα-S193D mice fail to restore the original mass. 70% of the livers were removed, and the percentage of growing livers was calculated at 3, 6, 9, and 15 days after PH. Bar graphs show summary of results obtained with 3 animals of each genotype per time point. Data shown are mean ± SD.

examined by Western blotting with specific Abs and by 2D-Western approach. Figure 4, A and B, shows that phosphorylation of C/EBPα at S193 is very weak in Hep3B2 cells and that cdc2 dramatically increases this phosphorylation. Although our data show that cdc2 phosphorylates C/EBPα at S193, it is possible that S21 of C/EBPα is also phosphorylated by cdc2.

We next determined whether the phosphorylation of C/EBPα at S193 might restore its growth inhibitory activity. These studies were performed in 2 cultured lines of hepatocytes: mouse Hepa1-6 and human Hep3B2 cells. These cells express relatively high levels of C/EBPα; however, they proliferate since C/EBPα is not phosphorylated in these cells (18–20). Therefore, we asked whether cdc2-mediated phosphorylation of C/EBPα in these cells might restore inhibitory activity of endogenous C/EBPα. Cells were transfected with pAdTrack-cdc2 plasmid, which expresses GFP and cdc2 from independent mRNAs. These studies showed that the ectopic expression of cdc2 inhibits proliferation of Hepa1-6 and Hep3B2 cells (Figure 4C; for Hepa1-6, see Supplemental Figure 5). To determine whether this inhibition requires C/EBPα, the expression of C/EBPα was inhibited by siRNA in cells transfected with cdc2 as shown in Figure 4C. We found that the inhibition of C/EBPα by siRNA eliminated the ability of cdc2 to stop proliferation of Hepa1-6 and Hep3B2 cells, while transfections with control siRNA did not change levels of C/EBPα and did not affect cdc2-mediated inhibition of cell proliferation. Thus, these studies revealed that cdc2 phosphorylates C/EBPα at S193 and restores its growth inhibitory activity in hepatoma cells.

In parallel studies, we examined the hypothesis that WT C/EBPα contributes to the arrest of cell division when hepatocytes finish the first round of cell division after PH. Particularly, we asked whether C/EBPα is hyperphosphorylated at 48 hours after PH when hepatocytes are finishing proliferation. 2D-Western approach showed that C/EBPα is phosphorylated at S193 in 48 hours after PH (Figure 4D). Examination of phosphorylation of C/EBPα by Western blotting with antibodies to ph-S193 showed that C/EBPα is phosphorylated at S193 in quiescent livers and in livers at 48 hours after PH (Figure 4F; C/EBPα IP). The increase of ph-S193 isoform at 48 hours after PH correlates with termination of hepatocyte proliferation. Since cyclin D3-cdk4 phosphorylates C/EBPα at S193 in the liver, we expected that this enzyme might be involved in the restoration of the inhibitory activity of C/EBPα. Therefore, we examined association of cdk4 with C/EBPα during the whole course of liver regeneration. Surprisingly, the interaction of C/EBPα with cdk4 was not detectable at 48 hours after PH (Figure 4F) despite the fact that C/EBPα is hyperphosphorylated at that time. Since cdc2 is elevated at 36–48 hours after PH (Figure 2D and Figure 4E), we reprobed the same filter with Abs to cdc2. Figure 4F shows that cdc2 is abundant in C/EBPα IPs at 48 hours after PH. The interactions of C/EBPα with cdc2 at 48 hours after PH was further confirmed by size exclusion chromatography (Supplemental Figure 4). Thus, these studies showed that cdc2 phosphorylates C/EBPα at S193 and, under normal conditions, increases its growth inhibitory activity. Under conditions of carcinogenesis, however, cdc2-mediated phosphorylation of C/EBPα leads to the degradation of C/EBPα via UPS (see below).

UPS degrades S193D mutant and ph-S193 isoform of C/EBPα by activation of gankyrin-mediated pathway. To determine pathways that degrade mutant S193D-C/EBPα and ph-S193 isoform of C/EBPα during DEN-mediated development of tumors, we inhibited proteasome activity by MG132 in C/EBPα-S193D mice treated by DEN/PB for 25 weeks. MG132 was injected in mice for 24 hours, and protein extracts were isolated and examined by Western blotting with antibodies to C/EBPα. The inhibition of proteasome activity led to the restoration of C/EBPα protein (Figure 5A). MG132 treatment also led to accumulation of higher MW forms of C/EBPα, which represent ubiquitin-C/EBPα conjugates. Examination of ubiquitin by direct Western blotting revealed a dramatic accumulation of total amounts of ubiquitin-protein conjugates in DEN/PB-treated mice (Figure 5A).

The specific degradation of ph-S193 and S193D isoforms of C/EBPα suggested that the liver cancer elevates expression of some proteins that recognize S193D and ph-S193 isoforms of C/EBPα. To identify these proteins, we performed glutathione S transferase (GST) pull-down experiments with GST-C/EBPα-S193D mutant. The initial studies were unsuccessful, since S193D mutant was degraded in nuclear extracts from DEN/PB-treated livers. Therefore, we included 10× excess of inhibitor of proteasome MG132 into the GST pull-down reactions. Several proteins were identified by mass spectroscopy analysis of GST pull-down samples of GST-S193D-C/EBPα. One of these proteins is gankyrin, which has been previously shown to be increased in livers of DEN/PB-treated animals (21). Gankyrin is a 25-kDa protein that was also identified as a subunit of 26S proteasome (22) and as the protein that causes activation of cdk4 by displacement of p16 from cdk4 (23). Given these activities of gankyrin, we asked whether gankyrin might be involved in the hyperphosphorylation of C/EBPα at S193 and in the proteasome-mediated degradation of C/EBPα. We first determined whether the interaction of gankyrin with C/EBPα requires phosphorylation of C/EBPα at S193. For this goal, GST pull-down assay was performed with S193A mutant and with phosphomimetic S193D mutant. Figure 5B shows that gankyrin interacts with S193D isoform of C/EBPα; however, no interaction was detectable with S193A mutant. We next examined expression of gankyrin in our animals at different time points after DEN/PB treatments. Western blotting revealed that expression of gankyrin was elevated at 6–10 weeks and then stayed at high levels throughout 35 weeks. The elevation of gankyrin correlated with the reduction of C/EBPα (Figure 5C). Examination of gankyrin mRNA confirmed the elevation of gankyrin in DEN/PB-treated mice. We next determined whether endogenous gankyrin interacts with WT C/EBPα in livers of DEN/PB-treated mice. Examination of C/EBPα IPs from nuclear extracts of different time points showed that gankyrin is associated with C/EBPα at 6 and 10 weeks and is not detectable in C/EBPα IPs at later time points since C/EBPα is degraded at this time (Figure 5D). We also examined the C/EBPα IPs with antibodies to cdk4 and found that cdk4 is also associated with C/EBPα (Figure 5D), suggesting that cdk4 might also be involved in the conversion of C/EBPα into S193-ph isoform.

The gankyrin-mediated displacement of p16^INK4A from cdk4 activates cdk4, which phosphorylates C/EBPα during DEN/PB-mediated carcinogenesis. Since previous studies implicated gankyrin in activation of cdk4 after DEN/PB treatments (23), we determined whether this activation of cdk4 might be involved in the conversion of C/EBPα into ph-S193 isoform. We first determined expression of cdk4, cyclin D3, and p16 after DEN/PB injections. Western blotting analyses showed that protein levels of cdk4 and cyclin D3 were increased at 20–30 weeks after DEN injection, while levels of p16 were reduced at these time points. The reprobe of p16 membrane with Abs to gankyrin confirmed the elevation of gankyrin in experimental mice (Figure 5E). These results showed that the interactions
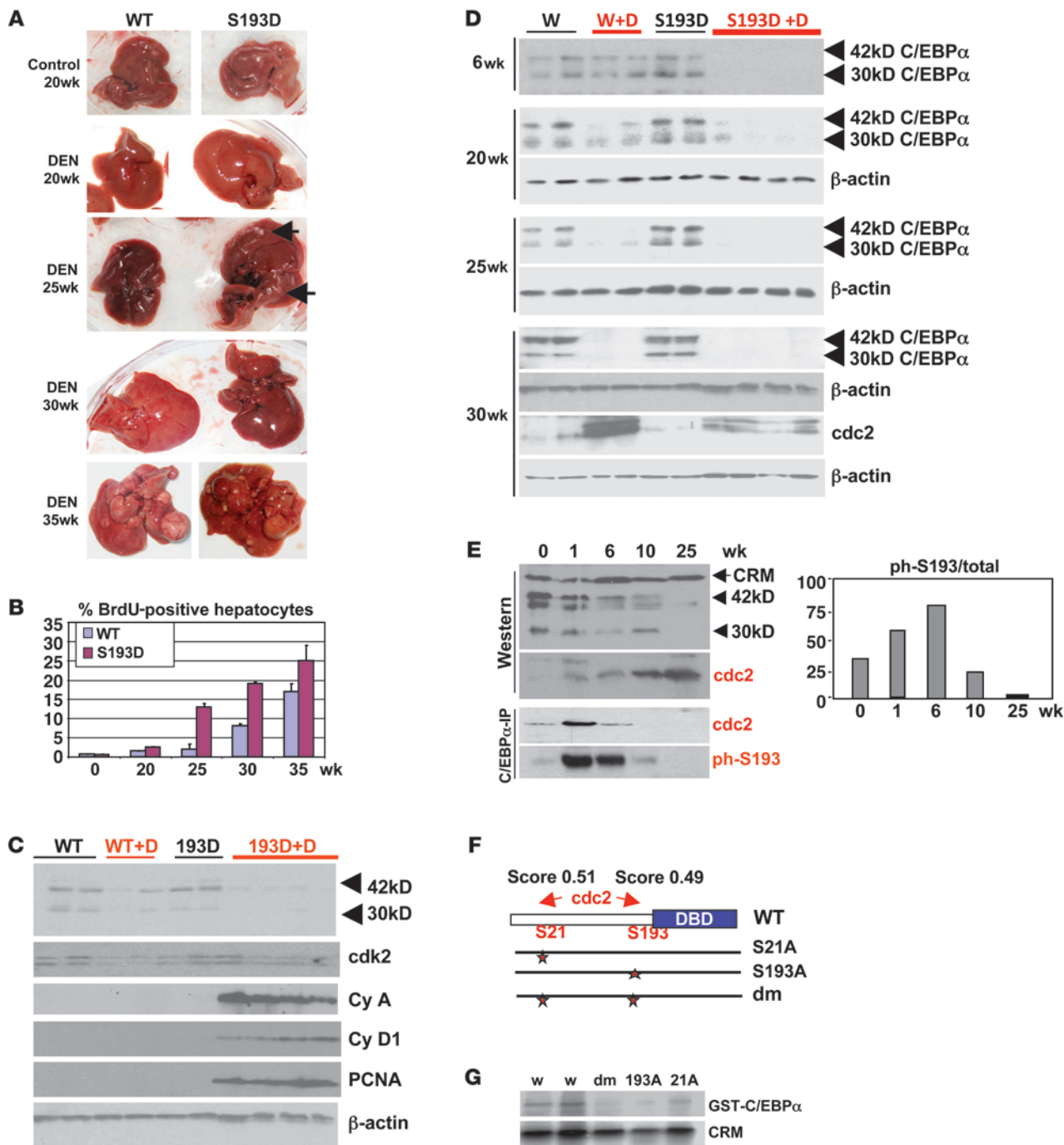
Figure 3
Development of tumors is accelerated in C/EBPα-S193D knockin mice. (**A**) Pictures of livers at different time points after DEN injection. Arrows show large tumor nodules observed in livers of mice treated with DEN for 25 weeks. (**B**) DNA synthesis is increased in livers of S193D mice. Bar graphs show percentage of BrdU-positive hepatocytes in tumor sections of livers of WT and S193D mice. Summary of results with 3 animals of each genotype is shown. Data shown are mean ± SD. (**C**) Expression of C/EBPα and cell-cycle proteins in WT and S193D livers at 25 weeks after DEN injection. Nuclear extracts were examined by Western blotting with antibodies shown on the right. (**D**) The mutant S193D isoform of C/EBPα is specifically degraded during liver tumor development. Western blotting was performed with WT and S193D livers at 6, 20, 25, and 30 weeks after injection of DEN. 2 isoforms of C/EBPα are shown by arrows. (**E**) cdc2 is elevated during DEN-mediated carcinogenesis and phosphorylates C/EBPα at S193 before degradation of C/EBPα. Western blotting was performed with nuclear extracts of WT mice. Bottom: C/EBPα was IP from nuclear extracts, and the IPs were probed with antibodies to cdc2 and ph-S193 C/EBPα. Bar graphs show a ratio of S193-ph isoform of C/EBPα to total C/EBPα protein. (**F**) Location of the predicted cdc2 sites within C/EBPα and generation of mutant constructs. (**G**) Cdc2 phosphorylates C/EBPα at S193 and S21. Cdc2 was IP from nuclear extracts isolated from the liver at 30 weeks after DEN treatments. Kinase assay was performed with WT C/EBPα and with C/EBPα mutants S21A, S193A, and S21A–S193A (Dm).
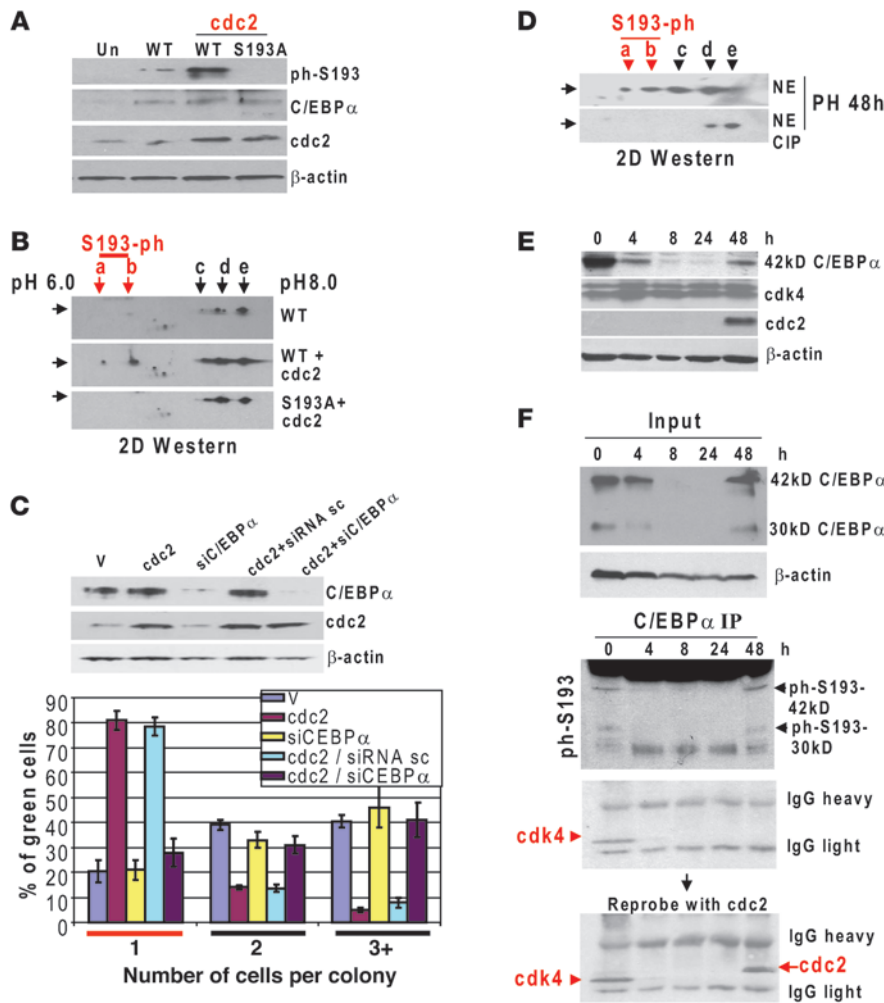
Figure 4
Cdc2 phosphorylates C/EBPα at S193 in Hep3B2 cells and restores growth inhibitory activity of C/EBPα. (**A**) Ectopic expression of cdc2 leads to phosphorylation of C/EPBα at S193. WT and S193A-C/EBPα were cotransfected with cdc2 into Hep3B2 cells. Expression of proteins was examined by Western blotting with antibodies to total C/EBPα, ph-S193-C/EBPα, cdc2, and β-actin. Un, untransfected cells. (**B**) Proteins were separated by 2D electrophoresis, transferred to the membrane, and probed with Abs to C/EBPα. Positions of ph-S193 isoforms (a and b) are shown by red arrows. (**C**) Cdc2 inhibits proliferation of Hep3B2 cells via restoration of growth inhibitory activity of C/EBPα. Hep3B2 cells were transfected with pAdTrack-cdc2, with pAdTrack-cdc2 plus siRNA to C/EBPα, and with pAdTrack-cdc2 plus scramble siRNA (control). Percentage of single cells (growth arrest) and proliferating cells was calculated. Upper image shows expression of C/EBPα and cdc2 in transfected cells. Data shown are mean ± SD. (**D**) C/EBPα is phosphorylated at S193 at 48 hours after PH. Nuclear extracts from livers at 48 hours after PH were examined by 2D gel Western blot approach. The bottom image shows 2D separation of the samples treated with alkaline phosphatase (CIP). (**E**) Expression of C/EBPα, cdk4, and cdc2 after PH. Western blotting was performed with the nuclear extracts isolated at different time points after PH. (**F**) Switch of interactions of C/EBPα with cdk4 to the interactions with cdc2 during liver regeneration. Upper image shows examination of C/EBPα in extracts used for the IP. Bottom image shows Western blotting of C/EBPα IPs with Abs to ph-S193 isoform of C/EBPα, cdk4, and cdc2. Heavy and light chains of IgGs are shown.

of cdk4 with C/EBPα were increased at 6 weeks; however, cdk4/cyc D3 levels were elevated at time points starting from 20 weeks. These differences suggested that there is an additional mechanism that activates cdk4 before the increase of cyclin D3-cdk4. Therefore, we next determined whether the elevation of gankyrin changes association of cdk4 with p16 and alters activity of cdk4 and its inter-

actions with C/EBPα. Cdk4 was IP from nuclear extracts, and the IPs were sequentially probed with Abs to gankyrin and to p16. Figure 5F shows that p16 is associated with cdk4 at 0 and 6 weeks; however, it is not detectable in cdk4 IPs at later time points after DEN/PB treatments. On the contrary, gankyrin is associated with cdk4 at 10–30 weeks after DEN/PB treatments. Examination of these cdk4 IPs in in vitro kinase reaction showed that kinase activity of cdk4 toward WT C/EBPα is much stronger at 6–35 weeks. This phosphorylation is specific for S193 because cdk4 does not phosphorylate the S193A mutant (Figure 5F). The lack of phosphorylation of S193A mutant by cdk4 is unlikely to be associated with the misfolding of the S193A mutant, because this mutant is highly active as transcriptional activator (19). Taken together, these studies showed that the elevation of gankyrin leads to the displacement of p16 from cdk4 and to activation of cdk4 toward C/EBPα.

Gankyrin triggers UPS-dependent degradation of S193D and S193-ph isoforms of C/EBPα. To further determine the role of gankyrin in the degradation of S193-ph and S193D isoforms of C/EBPα, we injected HA-tagged WT C/EBPα, C/EBPα-S193D, and C/EBPα-S193A mutants into control WT mice and into WT mice treated with DEN/PB for 25 weeks (which have increased levels of gankyrin) and examined stability of these proteins 3 days after injection. Western blotting with Abs to HA-tag showed that WT C/EBPα and S193D mutant are significantly reduced in DEN/PB-treated mice, while amounts of S193A mutant were not altered compared with amounts of this protein in untreated control mice (Figure 6A). These data clearly show that DEN/PB treatment triggers degradation of S193D and ph-S193D isoforms of C/EBPα in livers. To further examine the mechanisms of DEN-mediated reduction of S193D isoform of C/EBPα, we examined stability of WT and mutant C/EBPα in cultured HEK293 cells. The cells were treated with DEN and WT C/EBPα, and S193D and S193A mutants were transfected into these cells. The protein synthesis was blocked by cycloheximide (CHX), and the stability of

the transfected proteins was examined. While the half-life of WT C/EBPα was around 8 hours, the phosphomimetic mutation S193D reduced the half-life of C/EBPα to 2 hours. On the contrary, S193A mutation stabilized the protein (Figure 6B). We could not detect degradation of the S193A mutant within 16 hours. Investigation of longer time periods was complicated due to cell death.
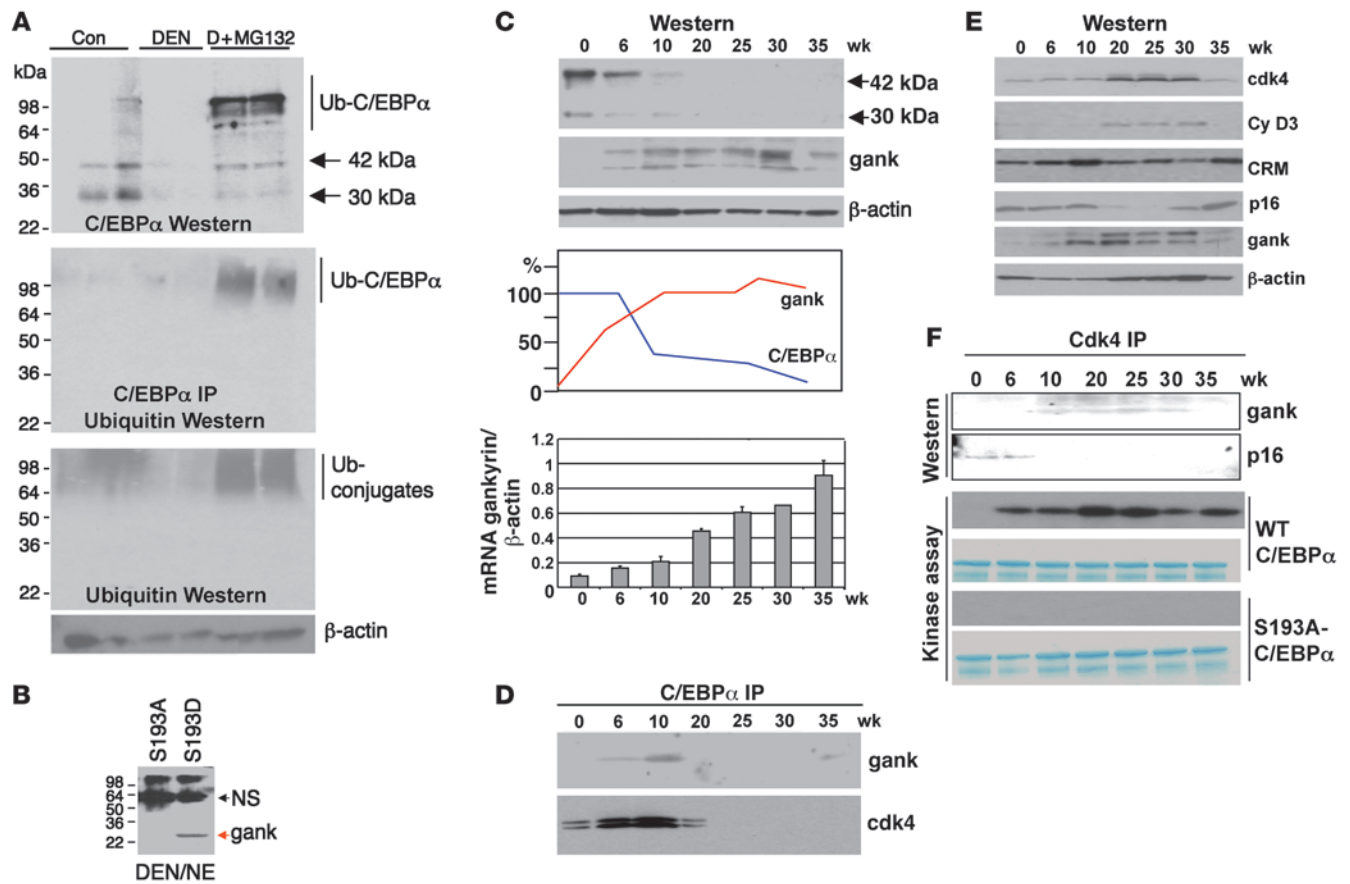
Figure 5
Elevation of gankyrin triggers degradation of C/EBPα by UPS. (**A**) Inhibition of proteasome blocks degradation of S193D C/EBPα in DEN-treated livers. Protein extracts of S193D untreated (Con), DEN-treated (for 25 weeks), and DEN-treated mice injected with MG132 were examined by Western blotting with Abs to C/EBPα and ubiquitin. Middle panel shows results of Western blotting of C/EBPα IP with antibodies to ubiquitin. Positions of C/EBPα isoforms and ubiquitinated conjugates are shown on the right. (**B**) Gankyrin preferentially interacts with S193D isoform of C/EBPα. GST-S193A and GST-S193D mutants were incubated with nuclear extracts isolated from livers of mice treated with DEN/PB for 25 weeks. (**C**) Expression of gankyrin is increased in livers of DEN/PB-treated mice. Upper image shows Western blotting with antibodies to C/EBPα and gankyrin. Middle image shows densitometric calculations of the levels of C/EBPα and gankyrin (gank). Bottom image shows levels of gankyrin mRNA determined by RT-PCR and calculated as a ratio to β-actin. Data shown are mean ± SD. (**D**) Gankyrin and cdk4 are associated with C/EBPα at early time points after DEN treatments. C/EBPα was IP from nuclear extracts and probed with antibodies to gankyrin and cdk4. (**E**) Expression of proteins that regulate activity of cdk4. Western blotting of nuclear extracts of DEN-treated mice was performed with antibodies shown on the right. (**F**) Gankyrin displaces p16 from cdk4 and activates cdk4. Cdk4 was IP from nuclear extracts and probed with Abs to gankyrin and to p16 (Western). The cdk4 IPs were examined in a kinase assay with WT C/EBPα and with S193A-C/EBPα as substrates (kinase assay).

The elevation of gankyrin in livers of DEN/PB-treated mice and its preferential interaction with S193D isoform of C/EBPα suggested that gankyrin might trigger UPS-mediated degradation of the S193D isoform of C/EBPα. To test this hypothesis, we set up a cotransfection system in which the degradation of C/EBPα was initiated by Ub-HA and it was determined whether gankyrin might accelerate degradation of the ubiquitinated form of C/EBPα. Figure 6C shows that cotransfection of WT C/EBPα with HA-Ub led to the accumulation of Ub-C/EBPα isoforms. While protein levels of 42-kDa C/EBPα were only slightly reduced in cells transfected with Ub-HA, the expression of gankyrin dramatically reduced both 42-kDa C/EBPα and Ub-C/EBPα conjugates (Figure 6C). We found that gankyrin triggered proteasome-dependent degradation of C/EBPα because inhibition of proteasome by MG132 abolishes the ability of gankyrin to reduce C/EBPα. We next performed similar studies with S193A mutant, which does not interact with gan-

kyrin. We found that although HA-Ub causes elevation of ubiquitinated C/EBPα-S193A isoforms, gankyrin is not able to trigger this mutant molecule for the UPS-mediated degradation (Figure 6D). Based on these data, we propose a mechanism by which cancer eliminates WT C/EBPα. According to our hypothesis, DEN/PB activates cdc2 and cdk4, which convert C/EBPα into ph-S193 isoform, and then gankyrin triggers UPS-mediated degradation of the ph-S193 isoform of C/EBPα (Figure 6E).

DEN/PB-mediated activation of gankyrin in old mice causes liver tumors at early time points due to fast elimination of the ph-S193-C/EBPα. Since the S193-ph isoform of C/EBPα represents more than 80% of the total protein in normal livers of old mice (15), one would assume that it might be eliminated quickly under conditions when expression of gankyrin is increased and that this elimination might lead to a faster development of tumors. To test this hypothesis, we treated 22-month-old mice with DEN/PB to increase expression of gan-
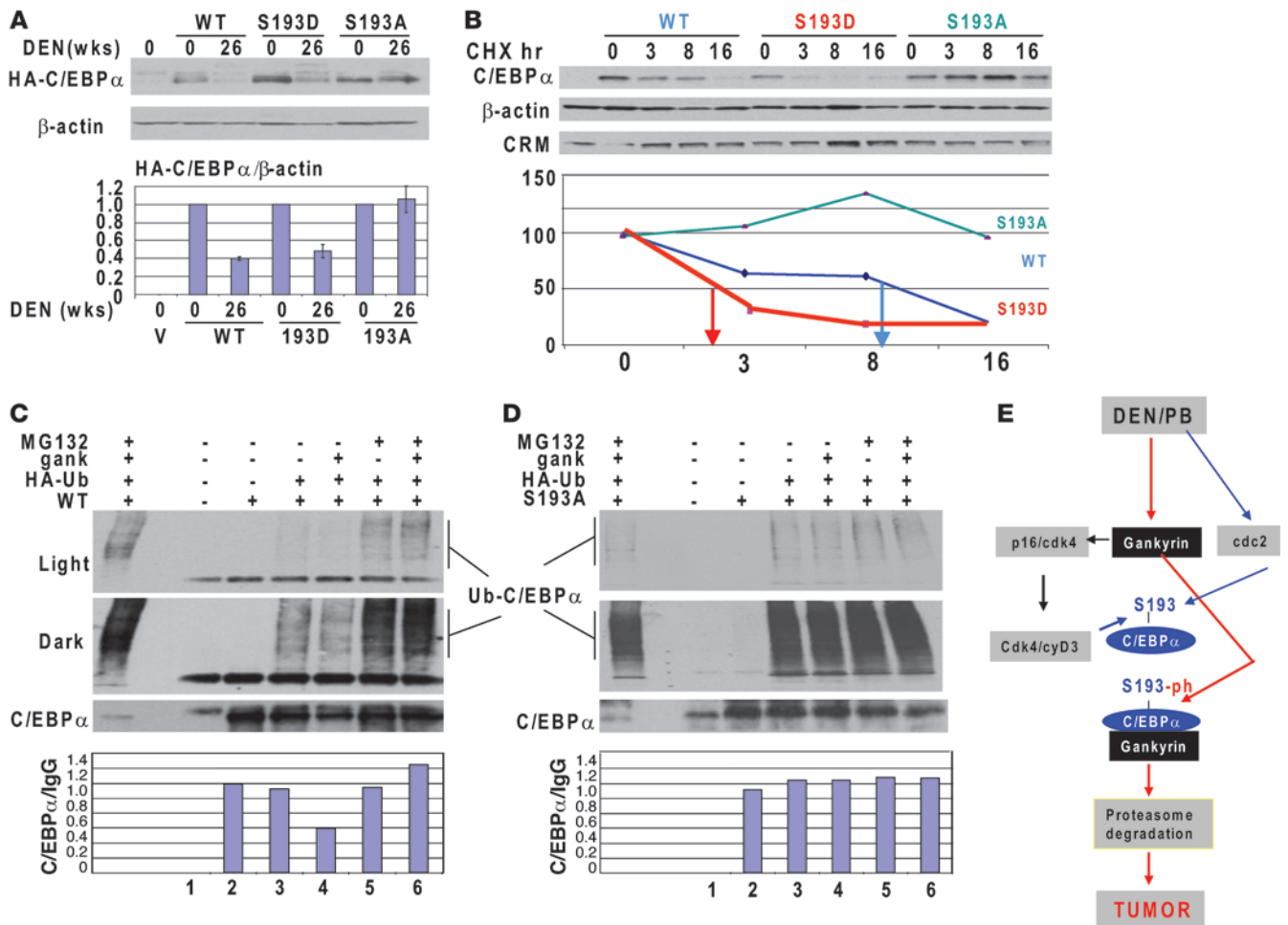
Figure 6

Gankyrin triggers UPS-mediated degradation of S193-ph isoform of C/EBPα in DEN/PB-treated mice and in cultured cells. (**A**) Mutation of S193 to Ala blocks degradation of C/EBPα in livers of DEN-treated mice. HA-tagged WT, S193D, and S193A mutant C/EBPα were injected in control and in DEN-treated mice; protein extracts were isolated 24 hours after injections and examined by Western blotting with Abs to HA-tag. Bar graphs show levels of C/EBPα calculated as ratio to β-actin. A summary of 2 experiments is shown. (**B**) Mutation of S193 to Asp reduces the half-life of C/EBPα, while mutation of S193 to Ala stabilizes C/EBPα in cells treated with DEN. C/EBPα proteins were transfected in HEK293 cells treated with DEN, protein synthesis was blocked by CHX, and the amounts of C/EBPα were determined by Western blotting. The bottom image shows densitometric calculations of C/EBPα levels. (**C** and **D**) Gankyrin triggers S193-ph isoform of C/EBPα to UPS-dependent degradation. WT C/EBPα (**C**) and S193A mutant (**D**) were cotransfected with HA-Ub and gankyrin in HEK293 cells. C/EBPα was IP and the IPs were examined by Western blot with antibodies to HA-tag and then with Abs to C/EBPα. Light and dark exposures for HA-tag Western blot are shown. Bar graphs show levels of C/EBPα calculated as ratio to IgGs. (**E**) A diagram showing pathways that convert WT C/EBPα into S193-ph isoform and pathways that trigger degradation of the ph-S193-C/EBPα during tumor development. Data shown are mean ± SD.

kyrin and to initiate carcinogenesis. Since old animals frequently have tumors, the animals were opened before the injection of DEN and tested for possible tumors. We focused examinations of liver proliferation on the animals at 12 and 20 weeks after DEN/PB injections, since old mice start to die at later time points. We initially examined expression of C/EBPα and gankyrin in mice treated for 12 weeks. Western blotting with 3 controls and 3 DEN/PB-treated animals of each age group showed that, although expression of gankyrin was increased in both young and old mice, the levels of elevation of gankyrin protein was higher in old mice (Figure 7, A and B). Examination of C/EBPα showed that, in young animals, C/EBPα was reduced to 50%, while C/EBPα was almost completely eliminated in livers of old mice (Figure 7, A and B). This elimination of C/EBPα took place at the protein level, since C/EBPα

mRNA was not changed by DEN/PB in young and old mice (Figure 7C). We next asked whether cdc2 was elevated in these mice and might contribute to the conversion of C/EBPα into ph-S193 isoform. We found that cdc2 was elevated in young and old livers by DEN/PB treatment (Figure 7A). Thus, these data show that the elevation of gankyrin in old mice leads to the fast and almost complete degradation of C/EBPα, while C/EBPα is degraded to a much lower degree in young mice. Our studies of young mice showed that the increase of rate of liver proliferation is a key step that takes place before appearance of the tumors and that S193D mice have an early increase in BrdU uptake (Figure 3B). Therefore, we determined DNA synthesis in young and old mice at 12 weeks after DEN/PB treatments. Figure 7D shows that only 2% of hepatocytes are BrdU positive in young mice at 12 weeks after DEN injection;
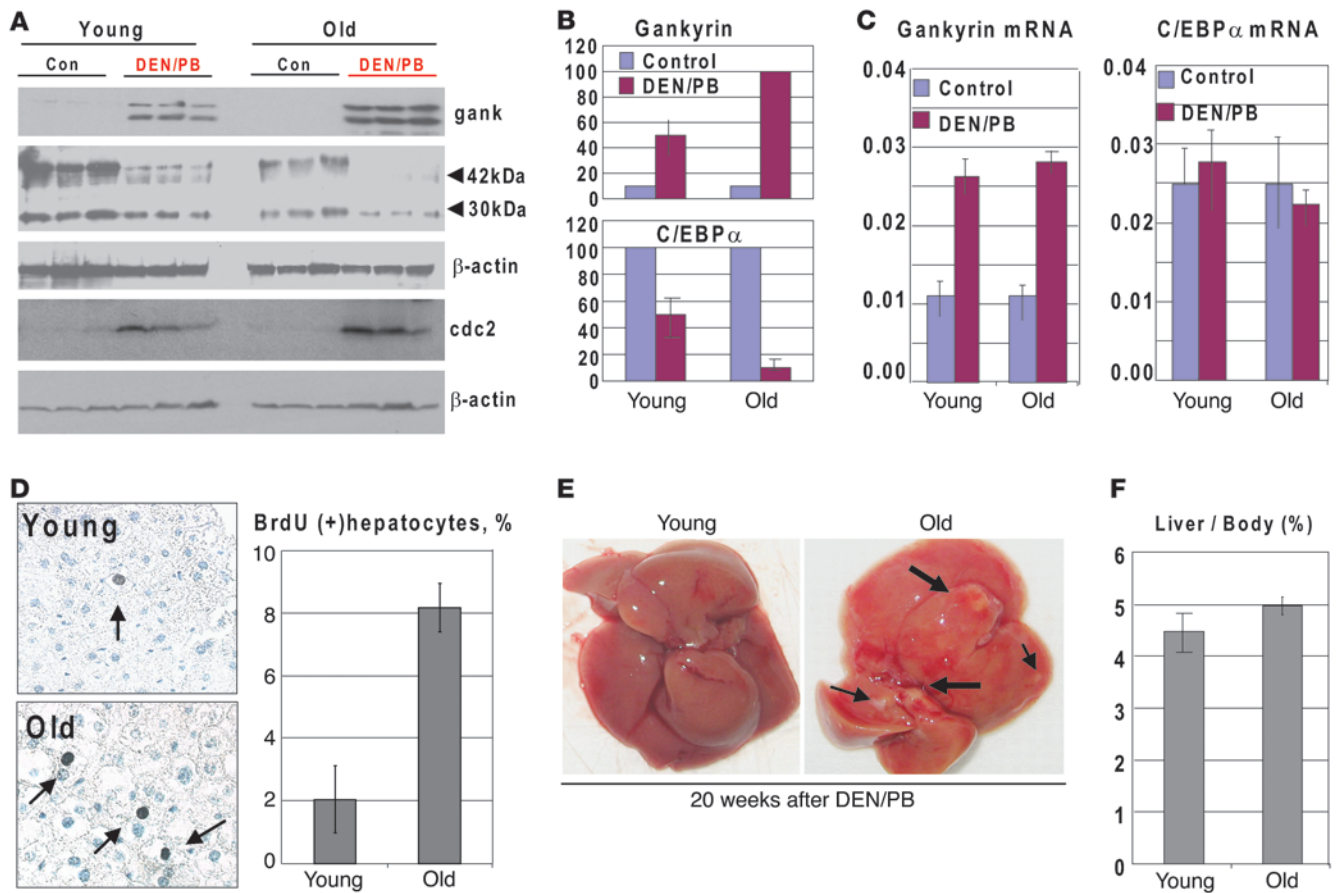
Figure 7
Treatment of old mice with DEN/PB initiates early liver proliferation and liver cancer via fast elimination of the ph-S193 isoform of C/EBPα. (**A**) Activation of gankyrin by DEN/PB in livers of old mice causes an early elimination of C/EBPα protein. Expression of C/EBPα, gankyrin, and cdc2 was examined by Western blotting with nuclear extracts from 3 mice of each age group. Positions of 42-kDa and 30-kDa isoforms of C/EBPα are shown. The membranes were reprobed with β-actin. (**B**) Levels of C/EBPα and gankyrin were calculated as ratios to β-actin. (**C**) Levels of gankyrin mRNA and C/EBPα mRNA were examined by RT-PCR and shown as ratios to β-actin mRNA. Bar graphs show a summary of 3 independent experiments. (**D**) DNA synthesis is increased in livers of old mice at 12 weeks after DEN/PB treatments. Left image shows a typical picture of BrdU staining of young and old livers. Arrows show BrdU-positive hepatocytes. Original magnification, ×63. Bar graphs present a summary of 3 experiments with 3 animals of each age group. (**E**) A typical picture of liver tumors in old mice at 20 weeks after DEN/PB treatments. Arrows show tumor nodules. (**F**) Liver body ratios in young and old animals at 20 weeks after DEN treatments. Data shown are mean ± SD.

however, up to 8% of hepatocytes proliferate in the old DEN/PB-treated mice. As shown in Figure 3B, this rate of liver proliferation (7%–8% BrdU-positive hepatocytes) is observed in young WT mice only at 30 weeks after DEN/PB treatments. Examination of livers at 20 weeks after DEN treatments showed that the development of tumor occurs early in livers of old mice, and it is detected at 20 weeks. Thus, these studies demonstrate that the aging liver is more susceptible to tumor development due to abundance of ph-S193 isoform of C/EBPα and due to a rapid elimination of the C/EBPα-S193-ph isoform by gankyrin-UPS pathway.

Age-associated spontaneous development of liver cancer is caused by gankyrin-mediated degradation of ph-S193-C/EBPα. Based on our results, we hypothesized that the spontaneous age-associated development of liver cancer might involve degradation of the ph-S193 isoform of C/EBPα. To test this hypothesis, we collected 4 samples of liver tumors from 30 animals of age 22–24 months. Examination of many young animals did not show tumor formation. Although

liver tumors in these 4 old animals differed, they were all neoplastic and included lymphoma, adenoma, and hepatocellular carcinoma. Supplemental Figure 6 shows a representative region of the large tumor in which the normal lobular architecture and portal tracts, including bile ducts, are not present. Hepatocytes are highly variable, with most containing cytoplasmic fat vacuoles or large eosinophilic protein globular inclusions and having hyperchromatic nuclei, with occasional atypical mitoses. We further confirmed that tumor sections have increased rates of proliferation by measuring BrdU uptake (Supplemental Figure 7).

Our studies of carcinogenesis in young WT mice showed that phosphorylation of C/EBPα at S193 is increased prior to the onset of the gankyrin elevation and development of liver cancer. Therefore, we asked whether the phosphorylation of C/EBPα at S193 might be also increased in livers of animals with tumors. Since ph-S193-C/EBPα is degraded by gankyrin in liver tumors, we examined phosphorylation status of C/EBPα in adjacent non-
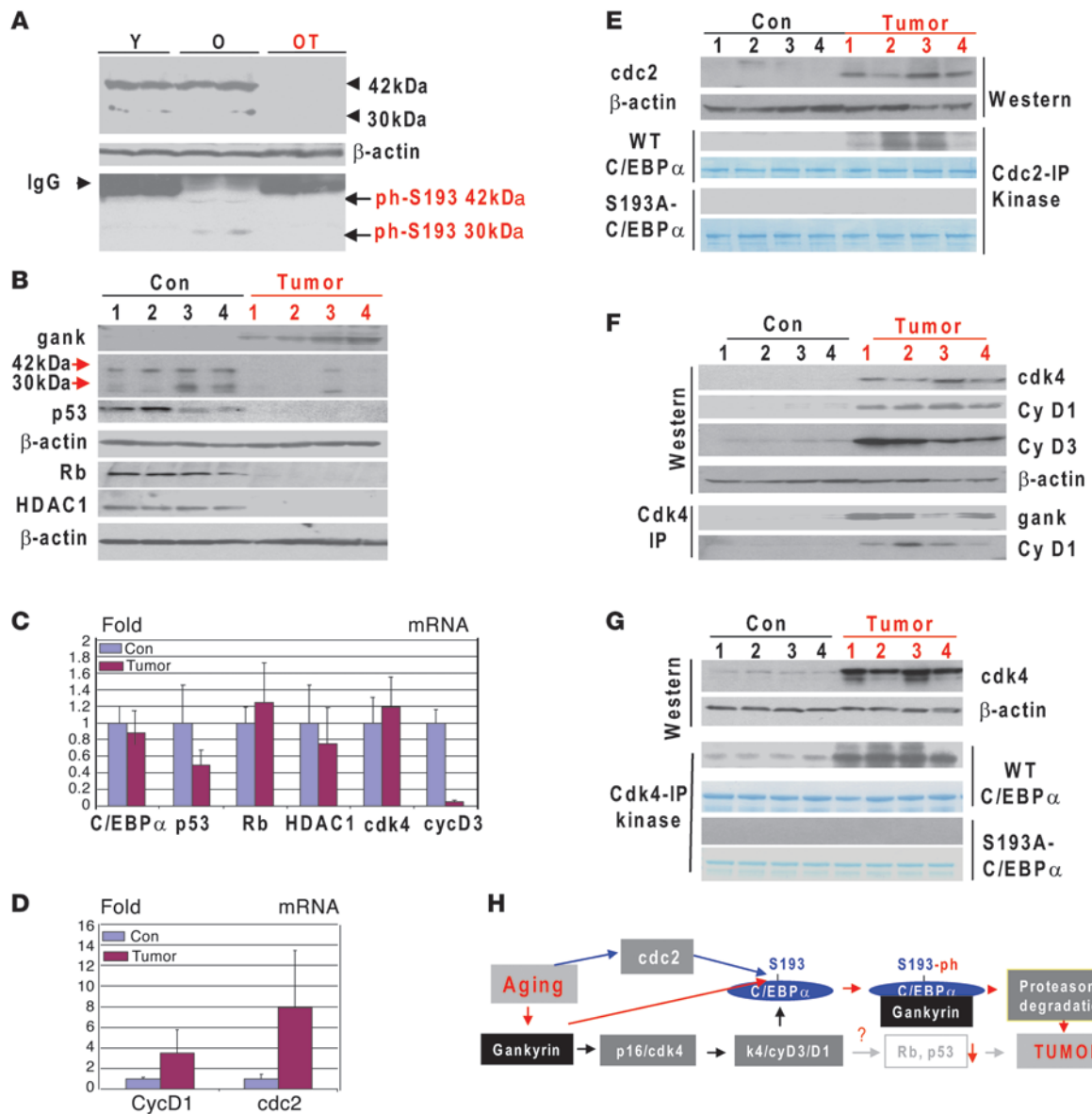
Figure 8

Age-associated liver cancer elevates gankyrin and eliminates C/EBPα. (**A**) C/EBPα is hyperphosphorylated in livers of old mice. Upper panel: Western blotting analysis of C/EBPα in nuclear extracts isolated from livers of young mice (Y), from healthy sections adjacent to liver tumors of old mice (O), and from liver tumors of old mice (OT). Bottom panel: C/EBPα was IP with antibodies to total C/EBPα and probed with antibodies to ph-S193 isoform of C/EBPα. (**B**) Gankyrin is elevated in liver tumors of old mice. Western blotting of proteins isolated from control mice and tumor sections was performed with Abs shown on the left. (**C** and **D**) Levels of mRNA coding for cell-cycle proteins. RT-PCR was performed with RNA isolated from control and tumor sections of old livers. (**E**) Cdc2 is increased in liver tumors. Western blotting was performed with Abs to cdc2. The membrane was reprobed with Abs to β-actin. Cdc2-IP:kinase: cdc2 was IP and examined in a kinase assay with WT and S193A mutant C/EBPα. (**F**) Cdk4 is activated in liver tumors of old mice. Western blotting was performed with antibodies shown on the right. Cdk4 was IP, and gankyrin and cyclin D1 were examined in these IPs. (**G**) Kinase activity of cdk4 toward C/EBPα is increased in tumor sections of the livers. Upper image shows input of cdk4 used for the IP. Cdk4 IPs were examined in a kinase assay with WT and S193A-C/EBPα as substrates. (**H**) A hypothetical model for the molecular basis of liver cancer in old mice. Data shown are mean ± SD.

tumor sections of the livers of old mice. We found that amounts of C/EBPα-ph-S193 isoform are dramatically increased in the adjacent nontumor sections, while total C/EBPα and ph-S193 isoform of C/EBPα were not detected in tumor sections due to degradation (Figure 8A). Thus, these data show that the hyperphosphorylation of C/EBPα at S193 is dramatically increased in nontumor sections of old mice adjacent to tumor sections.

We next examined expression of gankyrin in liver tumor sections and in livers of control animals of the same age and found that gankyrin was elevated in all tested liver tumor sections (Figure 8B). Consistent with data in Figure 8A, the levels of C/EBPα protein were dramatically reduced or undetectable in all tumor sections from old mice (Figure 8B). Real-time PCR was performed with RNA isolated from the same livers and detected a small reduction

of C/EBPα mRNA (Figure 8C). Since the elevation of gankyrin in DEN/PB-treated animals also causes degradation of p53 and Rb, we examined levels of these proteins in liver tumors. We found that p53 and Rb were dramatically reduced in tumor sections of the livers. In livers of old mice, ph-S193-C/EBPα isoform formed complexes with Rb and HDAC1 (17); therefore, we examined expression of HDAC1 and found a dramatic reduction of this protein in the tumor sections of the liver (Figure 8B). Examination of mRNA levels for p53, Rb, and HDAC1 showed that, while p53 mRNA was significantly reduced in tumors, the levels of Rb and HDAC1 mRNAs were not changed significantly (Figure 8C). Taken together, these studies show that 3 components of the C/EBPα-Rb-HDAC1 complex were eliminated in tumor sections of livers on the level of proteins, while levels of mRNAs were not changed.

We next determined kinases that might be activated in tumors of old mice and might be involved in the conversion of C/EBPα into ph-S193 isoform. Given our observations in DEN/PB-treated mice, we examined expression of cdc2 and found that this protein and its mRNA are elevated in tumor sections (Figure 8, D and E). Cdc2 was next IP and examined on the ability to phosphorylate C/EBPα at S193. Figure 8E shows that kinase activity of cdc2 toward WT C/EBPα was increased in liver tumors. This phosphorylation involves S193, since cdc2 does not phosphorylate S193A-C/EBPα mutant. Since cdk4 phosphorylates C/EBPα during DEN/PB-mediated carcinogenesis, we examined expression and activity of cdk4 as well as expression of proteins that regulate activity of cdk4. We observed a significant elevation of cdk4, cyclin D3, and cyclin D1 in liver tumors. Interestingly, only cyclin D1 was elevated on both mRNA and protein levels, while protein levels of cdk4 and cyclin D3 were elevated, but mRNAs not changed or reduced (Figure 8, C and D). Co-IP studies revealed that gankyrin and cyclin D1 were associated with cdk4 in tumors. Taking together the increase of cdk4-cyclin D1/D3 proteins and association of cdk4 with gankyrin, we inferred that cdk4 is activated in tumor sections. To further test this, cdk4 was IP and examined in in vitro kinase assay with C/EBPα substrate. Figure 8G shows that the kinase activity of cdk4 toward C/EBPα is much stronger in liver tumor sections. Experiments with WT and S193A mutant of C/EBPα showed that the activated cdk4 phosphorylated C/EBPα at S193. Based on these observations, we propose the following mechanisms of the age-associated development of cancer in the liver. Similar to DEN/PB, aging activates cdc2 and cdk4, leading to the complete conversion of C/EBPα into S193-ph isoform. This conversion leads to the interactions of ph-S193-C/EBPα with gankyrin, which delivers C/EBPα to proteasome-mediated degradation, leading to cancer (Figure 8H).

Discussion

C/EBPα is a strong inhibitor of liver proliferation. Proliferating livers neutralize growth inhibitory activity of C/EBPα by dephosphorylation at S193 (10, 15, 17). To determine whether the phosphorylation at S193 will protect livers from cancer, we generated C/EBPα-S193D knockin mice. Investigations of the liver proliferation after PH in C/EBPα-S193D mice have shown that the liver proliferation is dramatically inhibited by the phosphomimetic mutant of C/EBPα in young mice. These studies clearly demonstrated that C/EBPα should be dephosphorylated at S193 to allow liver proliferation. It is interesting to note that examination of C/EBPα-ΔPHR mice, in which S193 was deleted, did not find differences in liver proliferation in these animals compared with WT mice after PH (24). In light of our new data with the C/EBPα-S193D knockin mice,

it is clear that the lack of differences in liver proliferation between C/EBPα–ΔPHR and WT mice is associated with a neutralization of C/EBPα activity in livers of WT mice after PH by dephosphorylation at S193. In addition, the studies of liver regeneration in C/EBPα–ΔPHR mice have been limited to the analysis of a single time point, 48 hours after PH, which is not sufficient and does not show whether the whole course of liver regeneration is affected in these mice. Our studies of liver regeneration at several time points within 15 days after PH demonstrated that S193D mutant and ph-S193 isoforms of C/EBPα are strong inhibitors of liver proliferation and that proliferation of the liver requires dephosphorylation of C/EBPα or complete elimination of the protein. It is also important to note that studies of liver cancer in DEN/PB model of carcinogenesis and in liver cancer of old mice showed that C/EBPα needs to be degraded or neutralized to allow liver proliferation.

Liver cancer eliminates the "active" ph-S193 isoform of C/EBPα by activation of gankyrin-UPS pathways. Given the strong inhibition of liver proliferation by C/EBPα-S193D after PH, we expected that the C/EBPα-S193D mice should be resistant to liver cancer because C/EBPα-S193D cannot be neutralized by dephosphorylation. Surprisingly, we found that these animals became more sensitive to the development of liver tumors due to specific degradation of C/EBPα. Examination of cancer that naturally occurs in livers of old mice revealed a number of similarities in the molecular basis for the liver cancer in young mice under DEN/PB protocol and in livers of old mice (Figure 6E and Figure 8H). The key events of the cancer development include the following: (a) activation of cdc2 and cdk4 kinases, which completely convert C/EBPα into ph-S193 isoform, and (b) the elevation of gankyrin, which delivers ph-S193 isoform of C/EBPα to the proteasome to be degraded (see Figure 8H). In support of this hypothesis, we found that the treatments of old mice with DEN/PB also led to the faster elimination of ph-S193 isoform of C/EBPα and to the earlier development of tumors. It has been suggested that liver cancer might arise from the proliferation of transformed progenitor cells. Therefore, we examined the livers of S193D mice for expansion of progenitor cells. Immunostaining of the livers with markers of progenitor cells by double staining with α fetoprotein and cytokeratin 19 failed to detect a difference between WT and S193D livers (data not shown). This result suggests that the accelerated cancer in S193D mice is because of the loss of C/EBPα-mediated negative control in mature (differentiated) hepatocytes. During development of liver tumors, 2 kinases are involved in the conversion of C/EBPα into ph-S193 isoform: cdk4 and cdc2. The mechanisms of activation of cdc2 and cdk4 in liver tumor differ. While cdc2 is elevated by increase of *cdc2* mRNA, cdk4 is activated by stabilization of protein and by removing p16 from the cdk4. The identification of cdc2 as the enzyme that phosphorylates C/EBPα at S193 was quite surprising, since it also suggested that cdc2 might increase growth inhibitory activity of C/EBPα in livers that do not express gankyrin. In fact, we found that cdc2 does enhance growth inhibitory activity of C/EBPα at later stages of liver regeneration when livers have to stop division. Our data are consistent with previous observations showing the prooncogenic role of gankyrin in livers. Gankyrin is a small molecule (25 kDa), which also was discovered as 26S proteasome regulatory subunit p28 or p28[GANK] (21, 25). Further studies have shown that the expression of gankyrin is elevated in a number of hepatocellular carcinoma (HCC) (22). It has also been shown that the inhibition of gankyrin by siRNA reduces cell

growth (23). Little is known about mechanisms of gankyrin functions in HCC. It has been shown that gankyrin binds to MDM2/HDM2 and enhances ubiquitination and degradation of p53 (25, 26). Gankyrin contains the LACDE motif and interacts with Rb, leading to reduction of Rb (26). This interaction is involved in the conferring anchorage-independent growth on NIH 3T3 fibroblasts. In addition to the interaction with Rb, gankyrin also binds to cdk4 and displaces p16^{INK4a} from cdk4, leading to the activation of cdk4 (27). Our data revealed a new target for gankyrin — the active ph-S193 isoform of C/EBPα. The ph-S193 isoform of C/EBPα is associated in old livers with Brm, Rb, and HDAC1 (17). Our data show that liver tumors in old mice have reduced protein levels of 3 components of this complex: C/EBPα, Rb, and HDAC1. We suggest that gankyrin might trigger degradation of these proteins as components of the ph-S193-C/EBPα complexes. Although the reduction of Rb and p53 contributes to the liver cancer, the elimination of C/EBPα seems to be the most important event because the lack of C/EBPα in S193D mice after DEN/PB treatments leads to the earlier tumor development. An important question is how liver cancer activates gankyrin. Our data show that the levels of gankyrin mRNA are increased in liver tumors, suggesting the gankyrin promoter is activated by cancer. We are now examining mechanisms by which cancer activates the gankyrin promoter. In summary, we present molecular basis for the liver cancer that includes specific elimination of the growth inhibitory isoform of C/EBPα by gankyrin-UPS pathway. This information is quite significant because it will help to develop therapeutic approaches that might lead the protection of degradation of C/EBPα and to prevention of liver cancer.

Methods

Generation and genotyping C/EBPα-S193D knockin mice. C/EBPα gene is intronless. The C/EBPα-S193D mice were generated by replacement of the endogenous C/EBPα gene with knockin construct that contained a substitution of TC to GA in the position of S193 (see Figure 1A). This substitution led to the mutation of Ser to Asp and to alterations in restriction sites for MluI and BamH1. For experiments presented in this paper, we bred heterozygous mice and have examined WT, heterozygous, and homozygous mice from the same littermates. Experiments with animals have been approved by the Institutional Animal Care and Use Committee at Baylor College of Medicine (protocol AN-1439).

Antibodies and reagents. Antibodies to cyclin A, cyclin D1 (H-295), cdc2 (L-19), PCNA (FL-261), cdk4, Rb, p53, C/EBPα (14AA), gankyrin, and HA-tag were purchased from Santa Cruz Biotechnology Inc. Monoclonal anti–β-actin antibody was from Sigma-Aldrich. CHX and MG132 were from Sigma-Aldrich. BrdU uptake assay kit was from Invitrogen.

Kinase assay. Cdk4 and cdc2 were IP from nuclear extracts, and these IPs were examined in in vitro kinase assay as described (9, 15). WT C/EBPα and S193A-C/EBPα were used as substrates.

PH. PH was performed with 2-month-old WT and C/EBPα-S193D mice as described in our earlier publications (9, 15, 19). 70% of the liver was surgically removed, and regeneration was allowed to proceed for 8, 24, 36, 48, and 72 hours. Livers were collected and frozen in liquid nitrogen. Four animals at each time point after PH were examined.

Protein isolation and Western blotting. Nuclear extracts were isolated from cultured cells and from livers as described in previous papers (17–19). Nuclear extracts were isolated from mouse livers at 0, 8, 24, 36, 48, and 72 hours after PH, loaded on the gradient (4%–20%) PAAG, and analyzed by Western blotting.

Co-IP. C/EBPα or cdk4 was IP from nuclear extracts with polyclonal antibodies, and the presence of gankyrin, cdk2, and p16 in these IPs was examined by Western blotting with monoclonal antibodies to mentioned proteins.

BrdU uptake. BrdU was injected in animals 2 hours before animals were sacrificed. Livers were harvested and stained with antibodies to BrdU as described in our papers (18, 19).

DEN/PB protocol of liver carcinogenesis. Liver tumors were induced by DEN/PB tumor liver induction protocol as described (8). 5 μg DEN/g body weight was injected into WT and S193D mice, and then mice were provided with PB (0.05%) in drinking water. Animals were sacrificed at 6, 10, 20, 25, 30, and 35 weeks after DEN injection. Livers were harvested and analyzed as described above. Eight to ten animals of each genotype were used per time point.

Examination of gankyrin-mediated degradation of C/EBPα in mice and in cultured cells. For studies in animals, WT, S193D, and S193A C/EBPα were linked to HA-tag and the plasmids were injected in mice treated for 25 weeks with DEN/PB. Protein extracts were isolated in 24 hours and examined for expression of HA-C/EBPα using antibodies to HA-tag. For tissue culture studies, WT C/EBPα and S193A mutant were cotransfected with HA-ubiquitin and gankyrin into HEK293 cells, which express high levels of cyclin D3-cdk4 and phosphorylate WT C/EBPα at S193 (20). Protein extracts were isolated and C/EBPα was IP with polyclonal Abs. The IPs were probed with antibodies to HA-tag and with antibodies to C/EBPα.

Statistics. Bar graft data (mean ± SD) were generated by 2-tailed Student's *t* test from 3 independent experiments. Differences were considered significant at $P < 0.05$.

Address correspondence to: Nikolai A. Timchenko, Department of Pathology and Huffington Center on Aging, Baylor College of Medicine, One Baylor Plaza, Houston, Texas 77030, USA. Phone: 713.798.1567; Fax: 713.798.4161; E-mail: nikolait@bcm.tmc.edu.

1. Fausto N, Campbell JS, Riehle KJ. Liver regeneration. *Hepatology*. 2006;43(2 suppl 1):S43–S53.
2. Michalopoulos GK. Liver regeneration. *J Cell Physiol*. 2007;213(2):286–300.
3. Johnson PF. Molecular stop signs: regulation of cell-cycle arrest by C/EBP transcription factors. *J Cell Sci*. 2005;118(pt 12):2545–2555.
4. van den Heuvel S, Dyson NJ. Conserved functions of the pRB and E2F families. *Nat Rev Mol Cell Biol*. 2008;9(9):713–724.
5. Wang ND, et al. Impaired energy homeostasis in C/EBP alpha knockout mice. *Science*. 1995; 269(5227):1108–1112.
6. Flodby P, Barlow C, Kylefjord H, Ahrlund-Richter L, Xanthopoulos KG. Increased hepatic cell proliferation and lung abnormalities in mice deficient in CCAAT/enhancer binding protein alpha. *J Biol Chem*. 1996;271(40):24753–24760.
7. Timchenko NA, et al. CCAAT/enhancer binding protein alpha regulates p21 protein and hepatocyte proliferation in newborn mice. *Mol Cell Biol*. 1997;17(12):7353–7361.
8. Tan EH, Hooi SC, Laban M, Wong E, Ponniah AW, Wee A, Wang N. CCAAT/enhancer binding protein alpha knock-in mice exhibit early liver glycogen storage and reduced susceptibility to hepatocellular carcinoma. *Cancer Res*. 2005;65(22):10330–10337.
9. Wang H, et al. C/EBPalpha arrests cell proliferation through direct inhibition of Cdk2 and Cdk4. *Mol Cell*. 2001;8(4):817–828.
10. Timchenko NA. Aging and liver regeneration. *Trends Endocrinol Metab*. 2009;20(4):171–176.
11. Iakova P, Awad SS, Timchenko NA. Aging reduces proliferative capacities of liver by switching pathways of C/EBPalpha growth arrest. *Cell*. 2003; 113(4):495–506.
12. Porse BT, et al. E2F repression by C/EBPalpha is required for adipogenesis and granulopoiesis in vivo. *Cell*. 2001;107(2):247–258.

13. Pedersen TA, Kowenz-Leutz E, Leutz A, Nerlov C. Cooperation between C/EBPalpha, TBP/TFIIB and SWI/SNF recruiting domains is required for adipocyte differentiation. *Genes Dev*. 2001; 15(23):3208–3216.

14. Conboy IM, Conboy MJ, Wagers AJ Girma ER, Weisman IL Rando TA. Rejuvenation of aged progenitor cells by exposure to a young systemic environment. *Nature*. 2005;433(7027):760–764.

15. Wang GL, et al. Cyclin D3 maintains growth inhibitory activity of C/EBPalpha by stabilizing C/EBPalpha-cdk2 and C/EBPalpha-Brm complexes. *Mol Cell Biol*. 2006;26(7):2570–2582.

16. Muller C, Calkhoven CF, Sha X, Leutz A. The CCAAT/Enhancer binding protein alpha (C/EBPalpha) requires a SWI/SNF complex for proliferation arrest. *J Biol Chem*. 2004;279(8):7353–7358.

17. Wang GL, Salisbury E, Shi X, Timchenko LT, Medrano EE, Timchenko NA. HDAC1 cooperates with C/EBPalpha in the inhibition of liver proliferation in old mice. *J Biol Chem*. 2008;283(38):26169–26178.

18. Wang GL, Salisbury E, Shi X, Timchenko LT, Medrano EE, Timchenko NA. HDAC1 promotes liver proliferation in young mice via interaction with C/EBPalpha. *J Biol Chem*. 2008;283(38):26179–26187.

19. Wang GL, Iakova P, Wilde M, Awad SS, Timchenko NA. Liver tumors escape negative control of proliferation via PI3K/Akt-mediated block of C/EBPalpha growth inhibitory activity. *Genes Dev*. 2004;18(8):912–925.

20. Wang GL, Shi X, Salisbury E, Timchenko NA. Regulation of apoptotic and growth inhibitory activities of C/EBPalpha in different cell lines. *Exp Cell Res*. 2008;314(7):1626–1639.

21. Lim IK. Spectrum of molecular changes during hepatocarcinogenesis induced by DEN and other chemicals in Fisher 344 rats. *Mech Ageing Dev*. 2003;124(5):679–708.

22. Dawson SP. Hepatocellular carcinoma and ubiquitin-proteasome system. *Biochem Biophys Acta*. 2008;1782(12):775–784.

23. Li J, Tsai MD. Novel insights into the INK4-CDK4/6-Rb pathway: counter action of gankyrin against INK4 proteins regulates the CDK4-mediated phosphorylation of Rb. *Biochemistry*. 2002; 41(12):3977–3983.

24. Porse BT, et al. The proline-histidine-rich CDK2/CDK4 interaction region of C/EBPalpha is dispensable for C/EBPalpha-mediated growth regulation in vivo. *Mol Cell Biol*. 2006;26(3):1028–1037.

25. Higashitsuji H, et al. The oncoprotein gankyrin binds to MDM2/HDM2, enhancing ubiquitylation and degradation of p53. *Cancer Cell*. 2005;8(1):75–87.

26. Higashitsuji H, et al. Reduced stability of retinoblastoma protein by gankyrin, an oncogenic ankyrin-repeat protein overexpressed in hepatomas. *Nat Med*. 2000;6(1):96–99.

27. Li H, et al. Use of adenovirus-delivered siRNA to target oncoprotein p28GANK in hepatocellular carcinoma. *Gastroenterology*. 2005;128(7):2029–2041.